

## Supporting Information

### Lipid extraction by boron nitride nanosheet from liquid-ordered and liquid-disordered nanodomains

Yonghui Zhang<sup>1</sup>, Chun Chan<sup>1</sup>, Zhen Li<sup>1</sup>, Jiale Ma<sup>1</sup>, Qiangqiang Meng<sup>1</sup>, Xiaolin Cheng<sup>2</sup>  
and Jun Fan\*<sup>1,3,4</sup>

<sup>1</sup>Department of Materials Science and Engineering, City University of Hong Kong, 83 Tat Chee Avenue, Hong Kong, China. Correspondence and requests for materials should be addressed to J. F. (email: junfan@cityu.edu.hk)

<sup>2</sup>Division of Medicinal Chemistry and Pharmacognosy, College of Pharmacy, The Ohio State University, Columbus, OH 43210, USA

<sup>3</sup>Center for Advanced Nuclear Safety and Sustainable Development, City University of Hong Kong, 83 Tat Chee Avenue, Hong Kong, China

<sup>4</sup>City University of Hong Kong Shenzhen Research Institute, Shenzhen, China

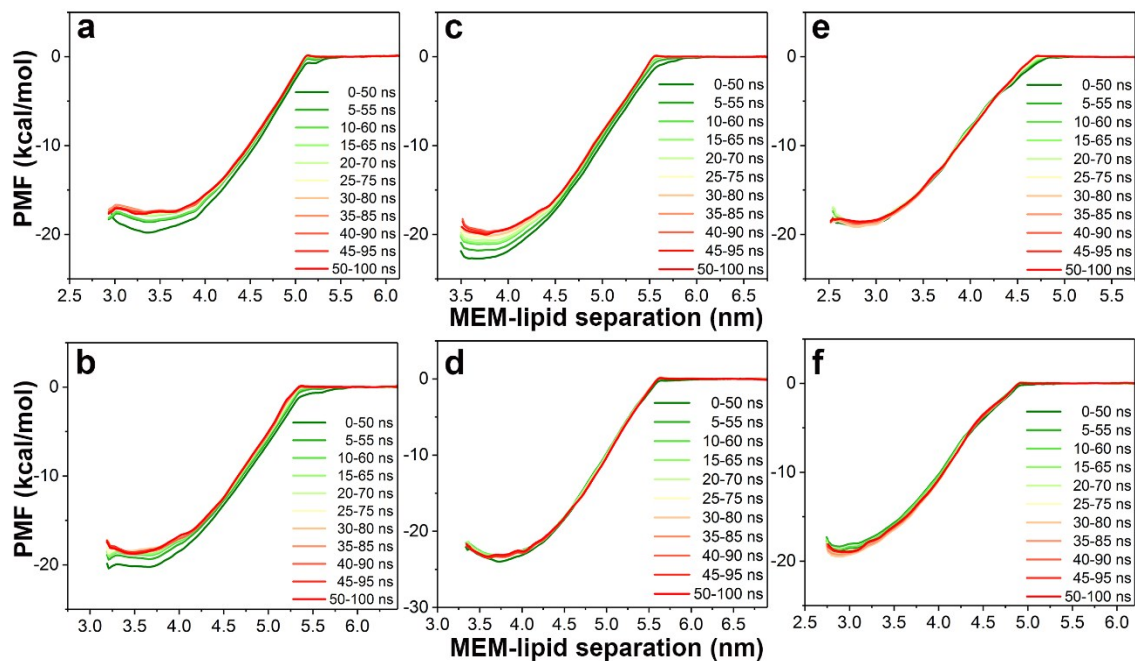


**Figure S1. Convergence of the US simulations for lipid molecules binding to the  $L_D$  membrane.** PMF profiles of POPC (a, b), DSPC (c, d), Chol (e, f) binding to  $L_D$  membrane with 5 ns intervals in 50 ns sliding blocks in US1 (upper panel) and US2 (lower panel).

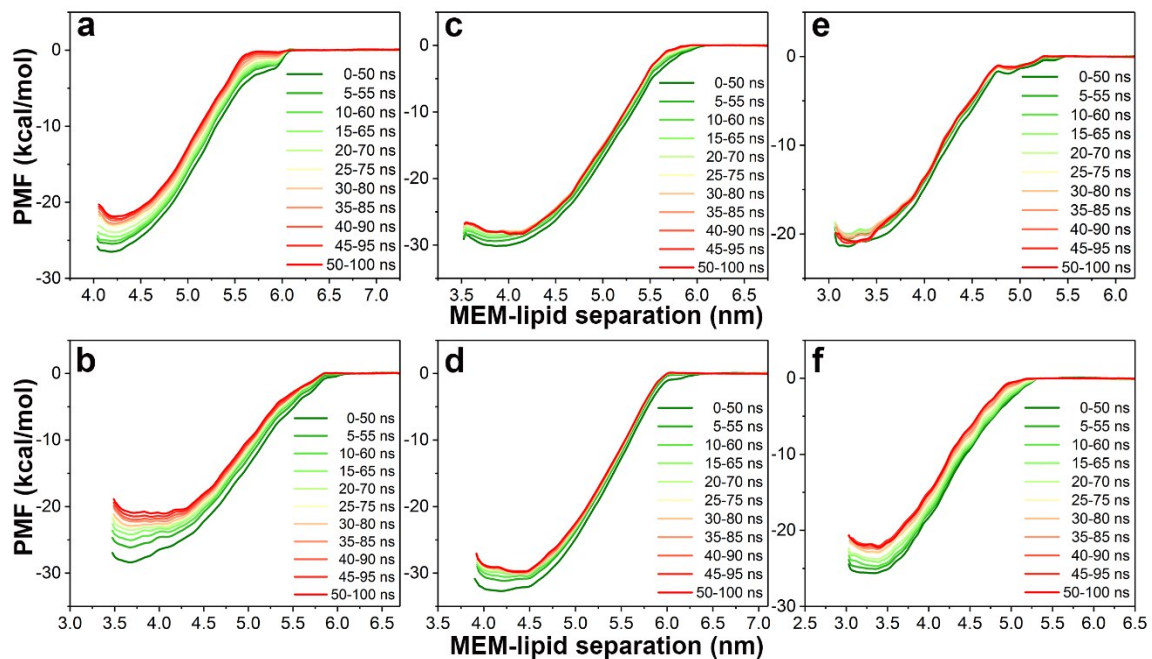


**Figure S2. Convergence of the US simulations for lipid molecules binding to the  $L_O$  membrane.** PMF profiles of POPC (a, b), DSPC (c, d), Chol (e, f) binding to  $L_O$  membrane with 5 ns intervals in 50 ns sliding blocks in US1 (upper panel) and US2 (lower panel).

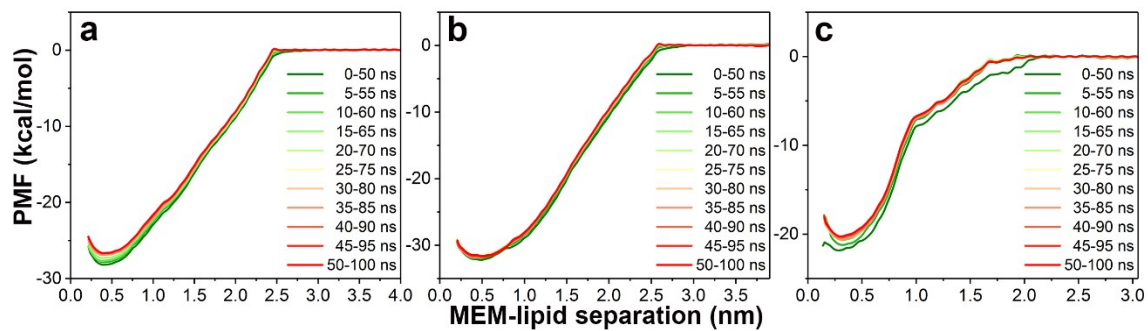


**Figure S3. Convergence of the US simulations for lipid molecules binding to the BNNS.** PMF profiles of POPC (a), DSPC (b), Chol (c) binding to BNNS with 5 ns intervals in 50 ns sliding blocks.

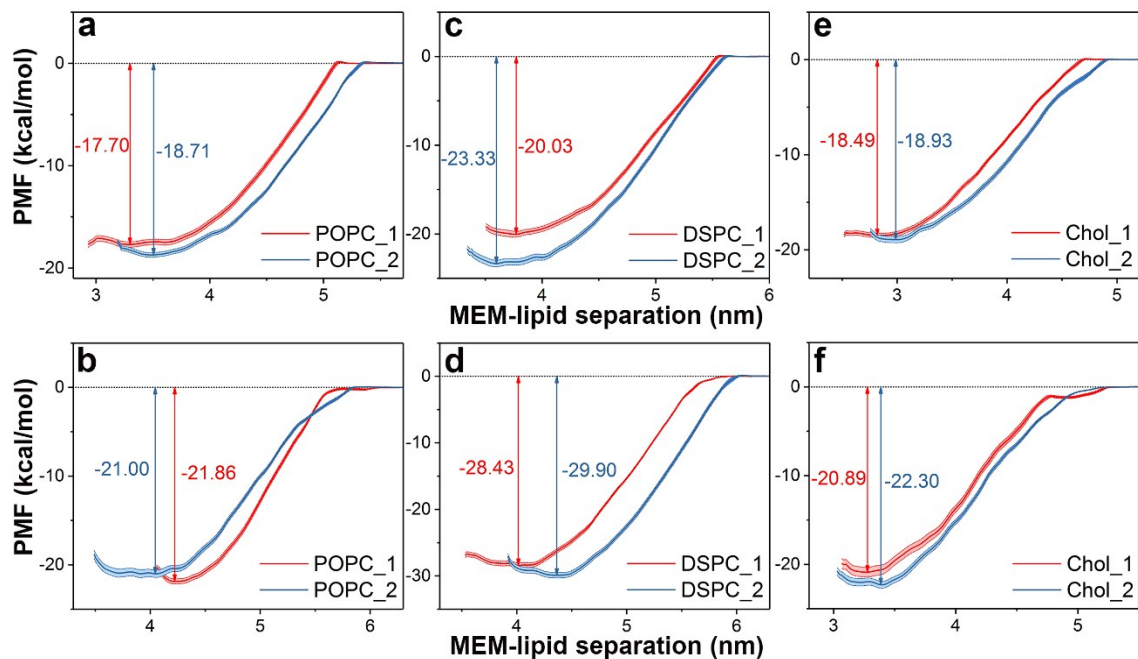


**Figure S4. Comparison of the PMF profiles for lipid molecules binding to  $L_D$ ,  $L_O$  membranes in US1 and US2.** PMF profiles of POPC (a), DSPC (c), Chol (e) binds to  $L_D$  membrane. PMF profiles of POPC (b), DSPC (d), Chol (f) binding to  $L_O$  membrane. Arrows indicate the position of PMF wells.

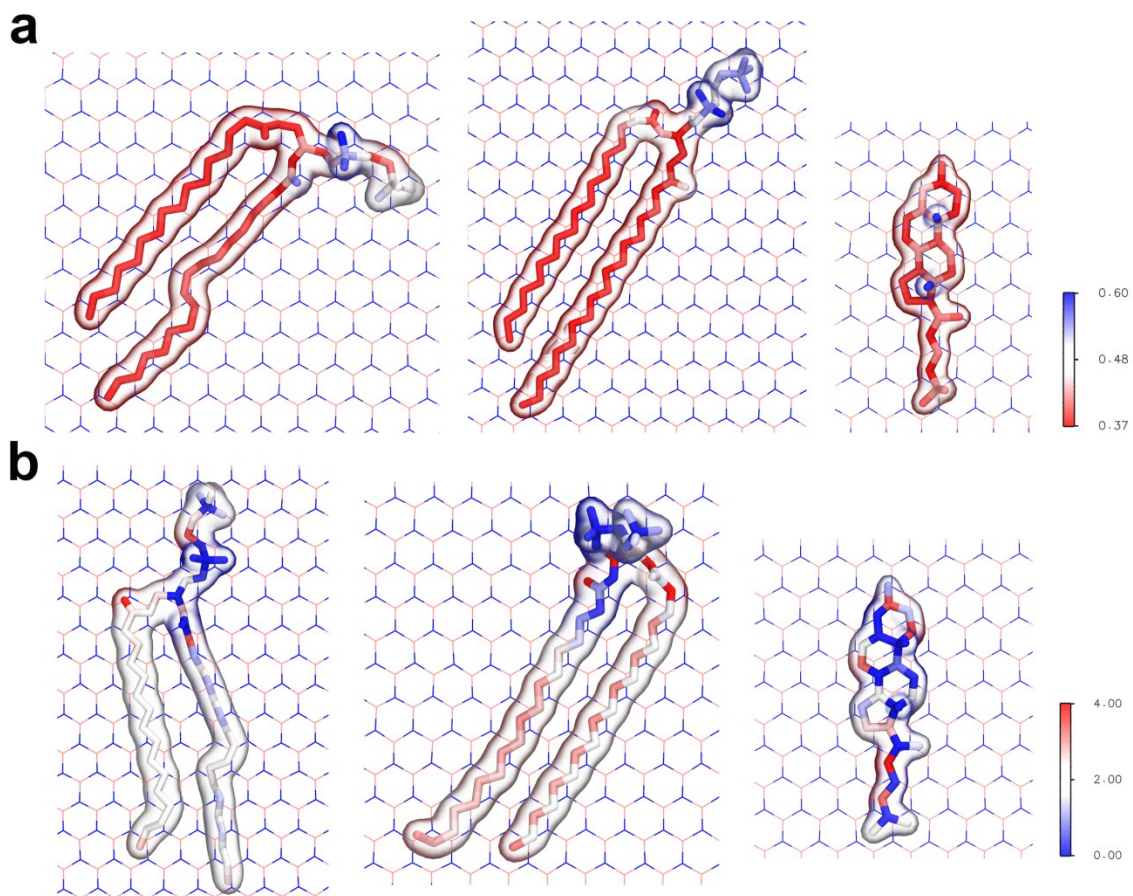


**Figure S5. Interaction strength of lipids binding to BNNS.** (a) Minimum distance between backbone atoms of lipids and BNNS mapping to the representative structures for POPC, DSPC and Cholesterol from left to right, respectively. (b) Number of contact between backbone atoms of lipids and BNNS mapping to the representative structures for POPC, DSPC and Cholesterol from left to right, respectively. A contact is defined when the distance of two atoms is less than 0.4 nm. The minimum distance and number of contact of each atom are listed in Table S1.

## Orientation switch during slow binding of Chol to BNNS

US simulations provide insights into the binding of Chol to BNNS that the Chol undergoes an orientation switch at a separation around 0.9 nm (Fig. S6a-b). According to the nomenclature of ring compounds proposed by Rose et al.<sup>45</sup>, the planar sterane backbone of cholesterol defines two distinct sides referred to as  $\alpha$  and  $\beta$  faces (Fig. S6c). The  $\alpha$  face displays a planar surface while the  $\beta$  face has a significantly rougher surface due to the presence of aliphatic groups. We found that during the binding/unbinding of Chol to BNNS, Chol binds BNNS with  $\alpha$  face (Fig. S6a state1) while the separation is less than 9 nm and switch to  $\beta$  faces binding (Fig. S6a state2) when the separation gradually increases. As the orientation of Chol switch, the slope of PMF becomes smoother. Conformational space defined by the separation and the orientation between Chol and BNNS clearly show the switching of two states (Fig. S6d).

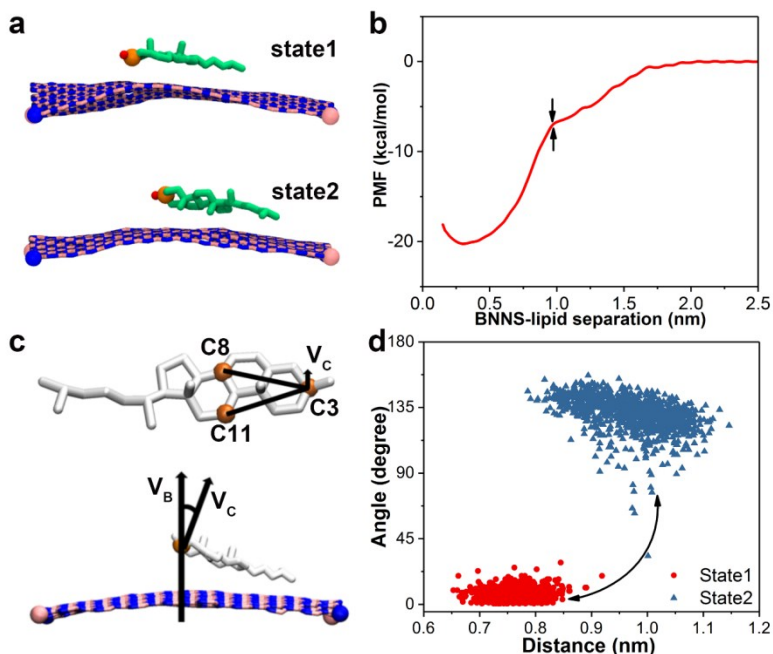


**Figure S6. US simulations reveal orientation switch during slow binding of Chol to BNNS.**

(a) Two state identified in US simulation near separation of  $\sim 0.9$  nm (b) PMF profile show the switch point (c) Orientation angle definition of Chol.  $V_C$  is defined as the cross product of  $V_{C3-C8}$  and  $V_{C3-C11}$ ,  $V_B$  is perpendicular to the BNNS plane point towards Chol,  $V_C$  and  $V_B$  determine the angle. (d) Conformational space of two identified states, which is defined by the separation and the orientation between Chol and BNNS.

## Assessment of the electrostatic interactions for BNNS

As we treated the BNNS in a simplified model using uncharged Lennard-Jones particles, to test whether the LJ potential can compensate the loss due to absence of electrostatic interactions, we compared the PMF of DSPC-BNNS systems with/without partial charges of  $-0.35e$  for the boron atoms and  $+0.35e$  for the nitrogen atoms of BNNS (Fig. S7). The well depth of system with/without partial charge are  $-33.63\pm 0.16$  kcal/mol and  $-31.59\pm 0.28$  kcal/mol, respectively, which counts for 6% shift of the well depth after adding the electrostatic interactions.

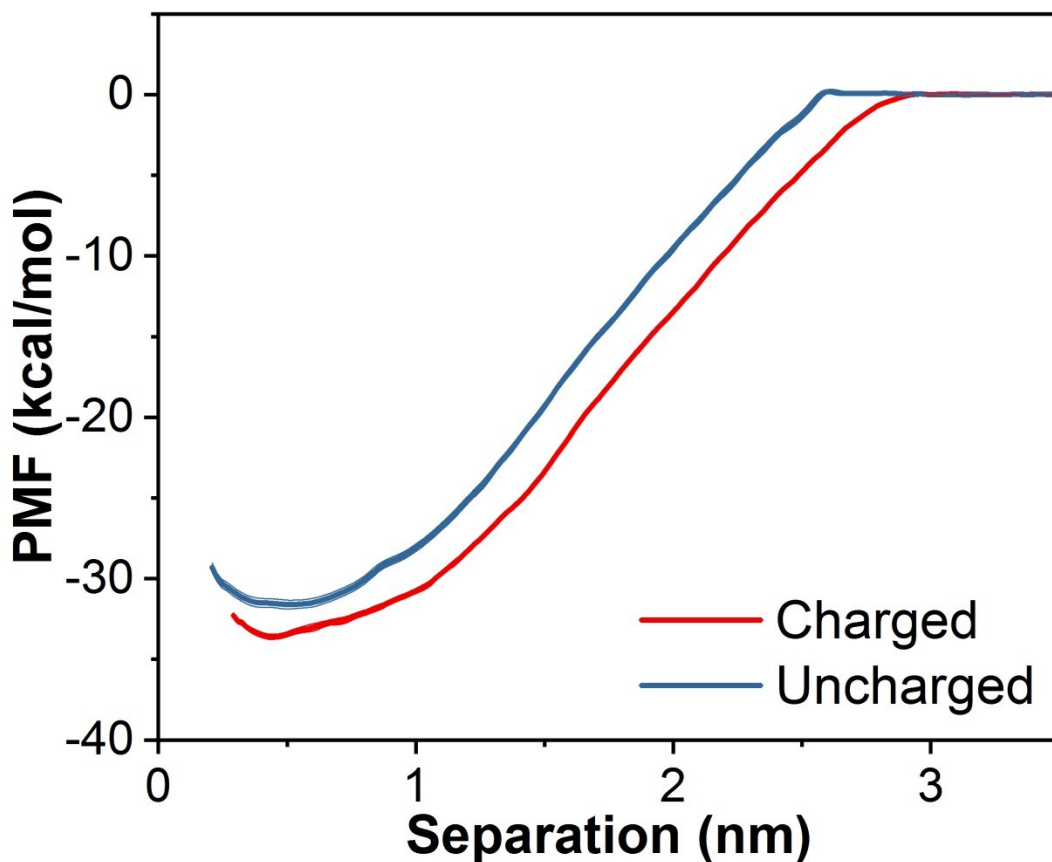


**Figure S7.** PMF of DSPC-BNNS system with/without partial charge of  $-0.35e$  (B) and  $+0.35e$  (N). The well depth of system with/without partial charge are  $-33.63\pm 0.16$  kcal/mol and  $-31.59\pm 0.28$  kcal/mol, respectively.

**Table S1. Binding strength of POPC, DSPC, and Cholesterol to BNNS.**

Atom Name	POPC		DSPC		Cholesterol		
	Min Distance (nm)	Contact Num.	Min Distance (nm)	Contact Num.	Min Distance (nm)	Contact Num.	Atom Name
N	0.477	0.295	0.549	0.065	0.377	2.98	C3
C12	0.428	2.309	0.548	1.451	0.402	1.007	O3
C13	0.477	1.94	0.559	1.103	0.452	0.007	C4
C14	0.498	1.471	0.531	0.518	0.434	0.051	C5
C15	0.51	1.329	0.559	1.005	0.39	1.508	C6
C11	0.393	3.508	0.473	1.828	0.38	2.812	C7
P	0.534	0.017	0.556	0.029	0.436	0.001	C8
O13	0.605	0.107	0.594	0.163	0.392	1.56	C14
O14	0.579	0.217	0.608	0.227	0.398	1.063	C15
O12	0.477	0.221	0.498	0.223	0.385	2.075	C16
O11	0.445	0.379	0.503	0.139	0.382	2.289	C17
C1	0.391	1.998	0.39	2.059	0.438	0.001	C13
C2	0.431	0.067	0.368	3.61	0.59	0	C18
O21	0.379	2.578	0.442	0.131	0.391	1.812	C12
C21	0.449	0.015	0.407	1.035	0.428	0.121	C11
O22	0.559	0	0.324	6.58	0.404	0.614	C9
C22	0.373	3.461	0.479	0.329	0.45	0	C10
C3	0.388	2.451	0.383	2.181	0.599	0	C19
O31	0.388	1.988	0.352	4.425	0.377	3.091	C1
C31	0.386	2.325	0.402	1.51	0.394	1.151	C2
O32	0.383	3.934	0.466	1.512	0.429	0.023	C20
C32	0.385	2.257	0.369	3.614	0.4	1.341	C21
C23	0.408	1.189	0.435	0.932	0.372	3.439	C22
C24	0.39	2.253	0.401	1.399	0.428	0.201	C23
C25	0.409	1.303	0.39	2.161	0.379	2.786	C24
C26	0.394	1.99	0.386	1.996	0.432	0.253	C25
C27	0.414	1.313	0.381	2.596	0.437	1.582	C26
C28	0.4	1.91	0.381	2.377	0.415	1.934	C27

C29	0.413	2.103	0.378	2.706	
C210	0.415	1.95	0.382	2.337	
C211	0.403	1.818	0.381	2.598	
C212	0.394	2.235	0.383	2.275	
C213	0.404	1.451	0.381	2.471	
C214	0.392	2.105	0.384	2.363	
C215	0.402	1.552	0.384	2.261	
C216	0.394	2.051	0.388	2.133	
C217	0.396	1.938	0.384	2.467	
C218	0.384	2.477	0.383	2.62	
C33	0.386	2.363	0.4	1.504	
C34	0.39	1.982	0.378	2.658	
C35	0.387	2.071	0.396	1.762	
C36	0.389	2.071	0.378	2.586	
C37	0.385	2.143	0.393	1.962	
C38	0.39	2.015	0.376	2.718	
C39	0.39	2.081	0.393	1.978	
C310	0.387	2.167	0.377	2.704	
C311	0.39	2.075	0.394	1.96	
C312	0.393	2.129	0.378	2.62	
C313	0.393	1.994	0.395	1.904	
C314	0.395	1.952	0.38	2.528	
C315	0.388	2.189	0.396	1.91	
C316	0.383	2.572	0.382	2.572	
C317			0.396	1.978	
C318			0.381	2.79	